Vortex dynamics on the surface of a torus: a review

Takashi SAKAJO
Department of mathematics, Kyoto University
Kyoto 606-8502, JAPAN
E-mail address: sakajo@math.kyoto-u.ac.jp

1 Introduction

For a 2D velocity field $(u_1(x,y), u_2(x,y))$ at $(x,y) \in \mathbb{R}^2$, the vorticity is defined by $\omega = \partial_y u_1 - \partial_x u_2$. Interactions among high vorticity regions give rise to various complicated flow patterns. For instance, when the fluid flow is subject to an external force in planar domains, these vorticity regions are localized and self-organizing into beautiful stationary lattice patterns [26, 28, 30]. Such vortex lattice structures, whose physical meaning varies depending on problems, are observed not only in fluid flows but also in the other physical phenomena such as superconductors in electromagnetic fields [2, 24], quantized vortex structures in superfluid helium [25, 64] and Bose-Einstein condensates [1, 22, 23] in low-temperature physics. In order to understand the formations of vortex lattices, we are tempted to create a phenomenological model based on the interactions among vortex structures. In this model, we assume that the potential function describing the interaction between two localized vortex structures has a logarithmic singularity, whose inducing azimuthal velocity field depends on the distance r and decays as $1/r$ as r goes to infinity. The model is different from process-driven partial differential equations such as the Navier-Stokes equations and the Ginzburg-Landau/Gross-Pitaevskii equations with localized vorticity initial data, but we can make use of it more flexibly to investigate the formation of vortex lattices for large number of high vorticity regions. A good survey of the model's history is given by Newton & Chamoun [46], in which many related references are found. See also a discussion in the Nobel Lecture by Abrikosov [3] regarding its physical relevance.

Suppose that the high vorticity regions concentrate in a finite set of isolated points. That is to say, the vorticity distribution is represented by Dirac's delta measures whose supports are defined on these points, called *point vortices*. Owing to the singular distribution, the vorticity is no longer a meaningful quantity since it diverges at the points, while the circulation for a small Jordan curve around the point is well-defined. Hence, we regard the circulations as the strengths of point vortices. For this vortex distribution, we can obtain a logarithmic interaction energy between two point vortices, thereby investigating the equilibrium states of point vortices, which are called *vortex crystals*. The study of vortex crystals in planar domains dates back to the "vortex atom" theory of matter by Thomson [61] more than a hundred year ago. Later, Campbell & Ziff [12] and Campbell & Kadtke [13] provided a catalogue of vortex crystals in a circular disc domain. Aref et al. [5] and Newton [42] survey the mathematical aspects of vortex crystals and give many vortex crystals in planar domains with/without boundaries, on a sphere and the hyperbolic plane. Fixed vortex equilibria in multiply connected circular domains are found in [52].

In the meantime, the search of vortex crystals is related to finding "good" point configurations that can be used for quadrature rules, computer designs and interpolation of functions in finite element schemes. A comprehensive review of the problem on point configurations is presented by

Hardin and Saff [31]. For a given particle-interaction energy function, one can define good point configurations as a local minimizer of the energy function. The most famous problem is finding a set of N points, $\omega_N = \{\boldsymbol{x}_i\}_{i=1}^N$, over d'-dimensional compact set A embedded in d-dimensional Euclidean space that minimizes the following Riesz s-energy.

$$\mathcal{E}_s(A,N) := \inf_{\omega_N \subset A} \sum_{i \neq j} |x_i - x_j|^{-s},$$

where $s > 0$ and $|\cdot|$ denotes the Euclidean distance. The parameter s controls the particle interaction. If $s = 1$, $\mathcal{E}_1(A,N)$ is the minimization for Coulomb energy corresponding to the classical potential theory of charged particles. As $s \to \infty$ with keeping N unchanged, this is equivalent to the best packing problem. On the other hand, for $s \to 0$, we obtain the minimizing problem of the following inter-particle energy,

$$\mathcal{E}_0(A,N) = \inf_{\omega_N \subset A} \sum_{i \neq j} \log |x_i - x_j|,$$

in which there appears an interaction energy with a logarithmic singularity. One of the central concerns in this problem is clarifying the behavior of $\mathcal{E}_s(A,N)$ as $N \to \infty$. According to [9, 10, 32]. we obtain $\mathcal{E}_s(A,N) = O(N^2)$ for $0 < s < d_H$ and $\mathcal{E}_s(A,N) = O(N^2 \log N)$ for $s \geqq d_H$ when points are on d-rectifiable compact manifolds with Hausdorff dimension d_H. Another minimizing energy problem in connection with quadrature rules on compact manifolds is considered by Damelin et al. [17, 18]. Point configurations on the surface of a sphere has also been well-investigated, since the problems of $s = \infty$ and $s = 0$ are related to Tammes problem [60] and Smale's seventh problem [57], respectively. In [45], a connection between vortex crystals and the optimal packings of the spherical surface is discussed. See also the the introduction and the references of this paper, regarding the applications to physical and biological problems.

The purpose of this article is reviewing the author's recent studies [53, 54, 55, 56] on vortex dynamics on the surface of a torus. Although the flows on the surface of a torus is no longer a physical relevance to real fluid flow phenomena, it is theoretically interesting to observe whether this geometric nature of the torus, which is a compact, orientable 2D Riemannian manifold with non-constant curvature and one handle, yields different vortex structures that are not observed so far. Vortex dynamics on the toroidal surface is not only an intrinsic theoretical extension in the field of classical fluid mechanics, but it would also be applicable to modern physics such as quantum mechanics and flows of superfluid films as discussed by Turner et al. [63]. As a matter of fact, a vector field of superfluid confined in a thin film on a toroidal surface has been considered analytically [14, 39]. A two-phase flow with a sharp interface on a torus was observed numerically in [48]. On the other hand, Hardin and Saff [31] showed some examples of point configurations on the surface of a torus that minimize Riesz s-energy: for $s \ll 1$, most of the points are distributed in the outer domain of the torus where the curvature is positive, while they spread uniformly for larger $s > 1$. The model of vortex dynamics proposed here adds more examples of point configurations on the toroidal surface in terms as vortex crystals [31].

The construction of the article is as follows. In Section 2, we provide the derivation of our vortex dynamics model based on the vorticity-streamline formulation. In Section 3, we consider the discrete vorticity distributions, i.e., point vortices, to investigate vortex crystals, whose linear stability and interactions are also discussed. In Section 4, we derive an analytic solution of a modified Liouville equation on the surface of a torus, which corresponds to a continuous vorticity distribution in the plane, known as the Stuart vortex [59]. The last section is summary and discussions.

2 Vortex dynamics on the surface of a torus

Let M be an orientable closed surface and g be the Riemannian metric on M. We derive the equation of vortex dynamics on the manifold (M, g) based on the mathematical formulation provided by Dritschel & Boatto [21]. We first consider a special Green's function $G_H(\zeta, \zeta_0)$ for $\zeta, \zeta_0 \in M$, called the *hydrodynamic Green's function*, satisfying

$$\nabla^2_M G_H(\zeta, \zeta_0) = \delta_{\zeta_0} - \frac{1}{\mathrm{Area}(M)}, \qquad G_H(\zeta, \zeta_0) = G_H(\zeta_0, \zeta),$$

where ∇^2_M and δ_{ζ_0} denote the Laplace-Beltrami operator and the dirac function at a point ζ_0 on (M, g) respectively. Analogous to vortex dynamics in the unbounded plane $\mathbb{R}^2$, the vortex dynamics on M is described in terms of the vorticity ω and the stream-function ψ. That is to say, for a vorticity distribution $\omega(\zeta)$, the stream-function $\psi(\zeta)$ satisfies Poisson's equation, $-\nabla^2_M \psi = \omega$. With the hydrodynamics Green's function, the solution is given by the following inversion formula.

$$\psi(\zeta) = -\int_M G_H(\zeta, \zeta_0)\omega(\zeta_0)\mathrm{d}\mu(\zeta_0), \tag{1}$$

where μ denotes the Riemannian volume form.

We shall construct the vortex dynamics when the vorticity distribution is given on the surface of a torus $\mathbb{T}_{R,r}$ of major radius R and minor radius r, which is embedded in the three-dimensional Euclidean space as follows [27].

$$\iota\colon (\theta, \phi) \in \mathbb{T}_{R,r} \mapsto ((R - r\cos\theta)\cos\phi, (R - r\cos\theta)\sin\theta, r\sin\theta) \in \mathbb{E}^3,$$

in which $(\theta, \phi) \in (\mathbb{R}/2\pi\mathbb{Z}) \times (\mathbb{R}/2\pi\mathbb{Z})$ is the toroidal coordinates in the latitudinal and the longitudinal directions. The modulus of the toroidal surface is given by $\alpha = R/r > 1$, from which we introduce the two real parameters $\mathcal{A}$ and ρ as $\mathcal{A} = \sqrt{\alpha^2 - 1} > 0$ and $\rho = \exp(-2\pi\mathcal{A}) \in (0, 1)$. On the other hand, the toroidal surface is endowed with a complex analytic structure through the following stereographic projection:

$$\zeta\colon (\theta, \phi) \in \mathbb{T}_{R,r} \mapsto \mathrm{e}^{i\phi} \exp\left(-\int_0^\theta \frac{du}{\alpha - \cos\theta}\right) \in \mathcal{D} \subset \mathbb{C},$$

in which $\mathcal{D} = \{\zeta \in \mathbb{C} \,|\, \rho < |\zeta| < 1\}$ is an annular domain. It is conveniently written as $\zeta = \mathrm{e}^{i\phi}\exp(r_c(\theta))$ by introducing

$$r_c(\theta) = -\int_0^\theta \frac{du}{\alpha - \cos\theta}.$$

This function is monotonically decreasing owing to $r_c'(\theta) < 0$ for $\alpha > 1$, satisfying a quasi-periodicity $r_c(\theta \pm 2\pi) = r_c(\theta) \mp 2\pi\mathcal{A}$. The Laplace-Beltrami operator $\nabla^2_{\mathbb{T}_{R,r}}$ for the toroidal surface is then expressed explicitly by using the toroidal coordinates (θ, ϕ) as follows:

$$\nabla^2_{\mathbb{T}_{R,r}} \equiv \frac{1}{r^2(R - r\cos\theta)}\frac{\partial}{\partial\theta}\left((R - r\cos\theta)\frac{\partial}{\partial\theta}\right) + \frac{1}{(R - r\cos\theta)^2}\frac{\partial^2}{\partial\phi^2}.$$

For the stream-function $\psi(\theta, \phi)$ and the vorticity distribution $\omega(\theta, \phi)$ on the toroidal surface, we consider Poisson's equation, $-\nabla^2_{\mathbb{T}_{R,r}}\psi = \omega$. By solving the equation, we can derive the incompressible velocity field $(u_\theta(\theta, \phi), u_\phi(\theta, \phi))$ on the toroidal surface as follows [27].

$$u_\theta(\theta, \phi) = \frac{1}{R - r\cos\theta}\frac{\partial\psi}{\partial\phi}, \qquad u_\phi(\theta, \phi) = -\frac{1}{r}\frac{\partial\psi}{\partial\theta}.$$

Since the toroidal surface is compact without boundaries, we take Gauss' constraint into considerations.

$$\iint_{\mathbb{T}_{R,r}} \omega d\sigma = 0, \tag{2}$$

where $d\sigma$ denotes the area element of the toroidal surface.

The analytic formula of the hydrodynamic Green's function $G_H(\zeta_1, \zeta_2)$ for $\zeta_1 = \zeta(\theta_1, \phi_1)$ and $\zeta_2 = \zeta(\theta_2, \phi_2)$ has been obtained [53]:

$$G_H(\zeta_1, \zeta_2) = \frac{1}{2\pi} \log \left| \zeta_2 P\left(\frac{\zeta_1}{\zeta_2}\right) \right| + \frac{1}{4\pi^2 \mathcal{A}} r_c(\theta_1) r_c(\theta_2) + F(\theta_1) + F(\theta_2) - \frac{1}{4\pi} r_c(\theta_1) - \frac{1}{4\pi} r_c(\theta_2), \tag{3}$$

in which the Schottky-Klein prime function $P(\zeta)$ associated with the domain $\mathcal{D}$ and the function $F(\theta)$ are given by

$$P(\zeta) = (1-\zeta) \prod_{n=1}^{\infty} (1-\rho^n \zeta)(1-\rho^n \zeta^{-1}), \qquad F(\theta) = -\frac{1}{4\pi\alpha^2} \int_0^{\theta} \frac{\alpha u - \sin u}{\alpha - \cos u} du. \tag{4}$$

Note that $G_H(\zeta_1, \zeta_2)$ is a doubly periodic function on the annular domain $\mathcal{D}$ with respect to the two arguments.

In this article, we consider the two types of vortex distributions. One is the singular vorticity distribution consisting of δ-measures at N points, called *point vortices*, which is given by

$$\omega(\zeta) = \sum_{m=1}^{N} \Gamma_m \delta_{\zeta_m}. \tag{5}$$

Here, $\zeta_m = (\theta_m, \phi_m) \in \mathbb{T}_{R,r}$ represents the location of the mth point vortex and the constant $\Gamma_m \in \mathbb{R}$ is its strength for $m = 1, \ldots, N$. Point vortex dynamics in the unbounded plane has been used to understand fundamental vortex interactions in flow phenomena. We can find many references in the books by Saffman [50] and Newton [42]. The motion of point vortices is also considered on surfaces that have various geometric features, and it reveals connections between the geometry of flow domains and fluid evolutions. One of the most important examples is the surface of a sphere. The evolution equation for point vortices on the spherical surface was derived by Bogomolov [8] and Kimura & Okamoto [33], which has been utilized as theoretical models of planetary flows on a sphere with/without rotation [19, 43, 58]. It is generalized in a unified manner to point vortex dynamics on surfaces with constant curvature by Kimura [34]. Hally [29] investigated the stability of vortex street with using a generalized vortex dynamics on symmetric surfaces of revolutions. Recently, Dritschel & Boatto [21] have considered point vortex dynamics on 2D surfaces conformal to the unit sphere based on a mathematical framework of [7]. The evolution equation of point vortices in multiply connected planar domains has been derived in [51], which is used to investigate many physical and engineering problems such as an ocean flow [40] and an efficient force-enhancing wing design with linear feedback control [41].

Another family of vortex distribution is the *Stuart*-type vortex, whose distribution is given by

$$\omega(\zeta) = c\mathrm{e}^{d\psi} + g(\zeta), \qquad c, d \in \mathbb{R} \qquad cd < 0. \tag{6}$$

The function $g(\zeta)$ is specified depending on the Riemannian manifold M. For instance, $g(\zeta) = 0$ when M is the unbounded plane, which gives rise to the classical Liouville equation. This equation appears not only in fluid dynamics but also in many problems of mathematical physics such as the field theory and plasma physics. Owing to the physical relevance, many exact solutions have

been obtained in [6, 11, 15, 38]. In fluid dynamics, it is regarded as a mathematical model of free shear layers. For instance, Stuart [59] obtained a periodic row of smooth vorticity distributions. On the surface of the unit sphere, Crowdy [16] extended the notion of Stuart vortex, in which the function $g(\zeta)$ is given by $g(\zeta) = 2/d$.

3 Dynamics of point vortices

3.1 The N-vortex system and its integrability

Suppose that the initial vorticity distribution is given by the linear combination of δ-measures (5) whose supports are located at $\zeta_m = \zeta(\theta_m, \phi_m)$ and strength are given by Γ_m for $m = 1, \ldots, N$. We then obtain the stream-function through the inversion formula (1).

$$\psi(\zeta) = -\int_M G_H(\zeta, \zeta_0) \sum_{m=1}^{N} \Gamma_m \delta_{\zeta_m} \mathrm{d}\mu(\zeta_0) = -\sum_{m=1}^{N} \Gamma_m G_H(\zeta, \zeta_m).$$

By allowing the point supports of the δ-measures to move according to their inducing velocity field, we are going to derive the evolution equation of point vortices. Since the stream-function has a logarithmic singularity in the neighborhood of point vortex, we remove the self-singularity, giving rise to the following modified stream-function [36, 37] associated with ζ_m:

$$\psi_m(\zeta_m) = -\sum_{j \neq m}^{N} \Gamma_j G_H(\zeta_m, \zeta_j) - \frac{1}{2}\Gamma_m R(\zeta_m),$$

where the function $R(\zeta_m)$, called the Robin function, is defined by

$$R(\zeta_m) = \lim_{\zeta \to \zeta_m} \left[G_H(\zeta, \zeta_m) - \frac{1}{2\pi} \log d(\zeta, \zeta_m) \right].$$

Here, $d(\zeta, \zeta_m)$ represents the geodesic distance between two points at ζ and ζ_m on the toroidal surface. According to [21, 36], the equation of motion of the mth point vortices at $\zeta_m(t)$ is derived by

$$\frac{d\zeta_m}{dt} = -2i\lambda^{-2}(\zeta_m, \overline{\zeta}_m) \frac{\partial \psi_m}{\partial \overline{\zeta_m}},$$

where $\lambda(\zeta, \overline{\zeta}) = (R - r\cos\theta)/|\zeta|$ denotes the conformal factor associated with the metric of the toroidal surface. The equation is explicitly written down as follows [53].

$$r^2(\alpha - \cos\theta_m)\frac{\mathrm{d}\theta_m}{\mathrm{d}t} = \mathrm{i}\sum_{j \neq m}^{N} \Gamma_j \left[\frac{K(\zeta_m/\zeta_j) - \overline{K(\zeta_m/\zeta_j)}}{4\pi} \right], \tag{7}$$

$$\begin{aligned} r^2(\alpha - \cos\theta_m)^2 \frac{\mathrm{d}\phi_m}{\mathrm{d}t} = {} & \sum_{j \neq m}^{N} \Gamma_j \left[\frac{K(\zeta_m/\zeta_j) + \overline{K(\zeta_m/\zeta_j)}}{4\pi} + \frac{\alpha\theta_m - \sin\theta_m}{4\pi^2\alpha} + \frac{r_c(\theta_j)}{4\pi^2\mathcal{A}} - \frac{1}{4\pi} \right] \\ & + \Gamma_m \left[\frac{\alpha\theta_m - \sin\theta_m}{4\pi^2\alpha} + \frac{r_c(\theta_m)}{4\pi^2\mathcal{A}} + \frac{1}{4\pi}\sin\theta_m \right], \end{aligned} \tag{8}$$

in which a special function $K(\zeta)$ is defined by $K(\zeta) = \zeta P_\zeta(\zeta)/P(\zeta)$. We call the system of ODEs the N-vortex system, which is formulated as a Hamiltonian system with N degrees of freedom with Hamiltonian

$$\mathcal{H}(\theta_1, \ldots, \theta_N, \phi_1, \ldots, \phi_N) = -\frac{1}{2}\sum_{m=1}^{N}\sum_{j\neq m}^{N}\Gamma_m\Gamma_j G_H(\zeta_m, \zeta_j) - \frac{1}{2}\sum_{m=1}^{N}\Gamma_m^2 R(\theta_m). \tag{9}$$

This contains the logarithmic particle-interaction energy $G_H(\zeta_m, \zeta_j)$ between the two point vortices at ζ_m and ζ_j. Under the theory of Hamiltonian dynamical systems, we can discuss the integrability of the system. Let I_N be defined by

$$I_N = \sum_{m=1}^{N}\Gamma_m(\alpha\theta_m - \sin\theta_m),$$

then we have the following results whose proofs are given in [53].

Proposition 3.1. *I_N is invariant in time and it is in involution with the Hamiltonian.*

Theorem 3.1. *The 2-vortex system is integrable for any vortex strengths.*

3.2 Equilibrium states of point vortices

We find equilibrium states of point vortices, i.e., vortex crystals, in which their relative configuration is unchanged. Let us rewrite the equations (7) and (8) in a simple form.

$$\dot{\theta}_m = \sum_{j\neq m}^{N}\Gamma_j F_{mj}(\theta_1, \ldots, \theta_N, \phi_1, \ldots, \phi_N), \tag{10}$$

$$\dot{\phi}_m = \sum_{j\neq m}^{N}\Gamma_j G_{mj}(\theta_1, \ldots, \theta_N, \phi_1, \ldots, \phi_N) + \Gamma_m H_m(\theta_1, \ldots, \theta_N), \tag{11}$$

in which $\cdot$ denotes the temporal derivative, and F_{mj}, G_{mj} and H_m are specified by

$$F_{mj} = \frac{i}{r^2(\alpha - \cos\theta_m)}\left[\frac{K(\zeta_m/\zeta_j) - \overline{K(\zeta_m/\zeta_j)}}{4\pi}\right], \tag{12}$$

$$G_{mj} = \frac{1}{r^2(\alpha - \cos\theta_m)^2}\left[\frac{K(\zeta_m/\zeta_j) + \overline{K(\zeta_m/\zeta_j)}}{4\pi\alpha} + \frac{\alpha\theta_m - \sin\theta_m}{4\pi^2\alpha} + \frac{r_c(\theta_j)}{4\pi\mathcal{A}} - \frac{1}{4\pi}\right], \tag{13}$$

$$H_m = \frac{1}{r^2(\alpha - \cos\theta_m)^2}\left[\frac{\alpha\theta_m - \sin\theta_m}{4\pi\alpha^2} + \frac{r_c(\theta_m)}{4\pi^2\mathcal{A}} + \frac{1}{4\pi}\sin\theta_m\right]. \tag{14}$$

Suppose that N point vortices form a relative equilibrium state rotating at a constant speed V_0 in the longitudinal direction, say, $\theta_m(t) = \vartheta_m$ and $\phi_m(t) = \varphi_m + V_0 t$. Then the substitution of the ansatz into the equations (10) and (11) yields the following algebraic equations for vortex crystals.

$$\sum_{j\neq m}^{N}\Gamma_j F_{mj}(\vartheta_1, \ldots, \vartheta_N, \varphi_1, \ldots, \varphi_N) = 0, \tag{15}$$

$$\sum_{j\neq m}^{N}\Gamma_j G_{mj}(\vartheta_1, \ldots, \vartheta_N, \varphi_1, \ldots, \varphi_N) + \Gamma_m H_m(\vartheta_1, \ldots, \vartheta_N) - V_0 = 0. \tag{16}$$

Let us remark that any vortex crystal is a critical point of the Hamiltonian function (9) containing the logarithmic particle interaction energy term. The vortex crystal becomes a local minimizer of the Hamiltonian $\mathcal{H}$ when the eigenvalues of the hessian of $\mathcal{H}$ are all pure imaginary, in other words, it is neutrally stable.

There are several ways to find the solutions of the equations (15) and (16). First, one can naively prescribe locations and strengths of point vortices, thereby confirming whether or not they satisfy (15) and (16). Since the locations of such point vortices are usually generated under the assumption that the configuration satisfies a certain discrete symmetry, most of the vortex crystals obtained by this approach become symmetric. The second approach is solving the algebraic nonlinear equations for given strengths using numerical solvers such as Newton's method. This allows us to obtain asymmetric vortex equilibrium states, which was used to construct vortex crystals in the unbounded plane [4].

The other approaches are based on the linear algebraic formulation of the equations (15) and (16). Suppose that we fix the locations (ϑ_m, φ_m) of N point vortices. Then the equations are regarded as a linear algebraic null equation $A\mathbf{\Gamma} = \mathbf{0}$, in which

$$A = \begin{bmatrix} 0 & F_{12} & \cdots & F_{1N} & 0 \\ F_{21} & 0 & \cdots & F_{2N} & 0 \\ \vdots & \vdots & \ddots & \vdots & \vdots \\ F_{N1} & F_{N2} & \cdots & 0 & 0 \\ H_1 & G_{12} & \cdots & G_{N1} & -1 \\ G_{21} & H_2 & \cdots & G_{2N} & -1 \\ \vdots & \vdots & \ddots & \vdots & \vdots \\ G_{N1} & G_{N2} & \cdots & H_N & -1 \end{bmatrix} \in \mathbb{R}^{(2N+1)\times(N+1)}, \qquad \mathbf{\Gamma} = \begin{bmatrix} \Gamma_1 \\ \Gamma_2 \\ \vdots \\ \Gamma_N \\ V_0 \end{bmatrix} \in \mathbb{R}^{N+1}.$$

Since the matrix A encodes the geometric information on the configuration of the point vortices, it is referred to as the *configuration matrix*. The solution vector $\mathbf{\Gamma}$ consists of the strengths of N point vortices and the latitudinal speed of rotation V_0. The linear equation has a non-trivial null space, if it satisfies $\det(A^T A) = 0$. Hence, if we find the locations of N point vortices whose corresponding configuration matrix satisfies $\mathrm{Rank}(A) = k < N + 1$, then the vector $\mathbf{\Gamma}$ belongs to $N + 1 - k$ dimensional null space. When $k = 1$ in particular, we can identify the strength Γ_m of the mth point vortex uniquely up to $\pm$ sign under a certain normalization condition. The null space of A is numerically constructed by the singular value decomposition, which is a standard numerical tool. In the third approach, prescribing the locations of point vortices, we check if the configuration matrix A becomes rank-deficient. In the fourth method, we use a stochastic method, called the *Brownian ratchets*, where vortex crystals are searched by generating a random walk of points until its corresponding configuration matrix becomes rank-deficient. This method was proposed by Newton and Chamoun [44], which was successfully applied to produce many symmetric and asymmetric point vortex equilibria in the unbounded plane [44] and on the spherical surface [45, 47].

In what follows, we show a catalogue of vortex crystals obtained through these approaches. The first approach yields several vortex crystals on the toroidal surface [53]. When point vortices are located at antipodal points, the configuration is a vortex crystal for any strengths. As a matter of fact, it is a fixed equilibria, which is a vortex crystal with $V_0 = 0$. When N identical point vortices are equally spaced along the line of latitude Θ_0, i.e.

$$\vartheta_m = \Theta_0, \qquad \varphi_m = 2\pi m/N, \qquad \Gamma_m = \Gamma, \qquad m = 1, \cdots, N, \tag{17}$$

then it is a vortex crystal, called the (latitudinal) N-ring [53].

Proposition 3.2. *Let $V_N(\Theta_0)$ be defined by*

$$V_N(\Theta_0) = \frac{N\Gamma}{(R - r\cos\Theta_0)^2}\left[\frac{\alpha\Theta_0 - \sin\Theta_0}{4\pi^2\alpha} + \frac{r_c(\Theta_0)}{4\pi^2\mathcal{A}}\right] + \frac{\Gamma\sin\Theta_0}{4\pi(R - r\cos\Theta_0)^2}.$$

Then the N-ring along the line of latitude Θ_0 is a relative equilibrium rotating in the longitudinal direction at the speed $V_N(\Theta_0)$.

Suppose next that two M-rings with the vortex strengths of the opposite signs are aligned along two symmetric lines of latitudes, namely Θ_1 and Θ_2 with $\Theta_1 + \Theta_2 = 2\pi$. Then, the locations of $N = 2M$ point vortices with the strengths $\Gamma_{2m-1} = \Gamma$ and $\Gamma_{2m} = -\Gamma$ are specified by

$$\theta_{2m-1} = \Theta_1, \qquad \phi_{2m-1} = \frac{2\pi}{M}m, \qquad \theta_{2m} = 2\pi - \Theta_1, \qquad \phi_{2m} = \frac{2\pi}{M}m, \tag{18}$$

and

$$\theta_{2m-1} = \Theta_1, \qquad \phi_{2m-1} = \frac{2\pi}{M}m, \qquad \theta_{2m} = 2\pi - \Theta_1, \qquad \phi_{2m} = \frac{2\pi}{M}m + \frac{\pi}{M}, \tag{19}$$

for $m = 1, \ldots, M$. The configuration (18) corresponds to M vortex dipoles, while the configuration (19) is called a *staggered pair of M-rings*. They are vortex crystals, which correspond to von Kármán vortex streets on the surface of a torus.

Proposition 3.3. *Let $r_e = \exp(r_c(\Theta_1) - r_c(2\pi - \Theta_1))$ and $V_M^d(\Theta_1)$ be defined by*

$$\begin{aligned} V_M^d(\Theta_1) &= -\frac{\Gamma}{(R - r\cos\Theta_1)^2}\sum_{j=1}^{M}\left[\frac{K(r_e\exp(i\frac{2\pi}{M}j)) + K(r_e\exp(-i\frac{2\pi}{M}j)) - 1}{4\pi}\right] \\ &\quad + \frac{M\Gamma(r_c(\Theta_1) - r_c(2\pi - \Theta_1))}{4\pi^2\mathcal{A}(R - r\cos\Theta_1)^2} + \frac{\Gamma\sin\Theta_1}{4\pi(R - r\cos\Theta_1)^2}. \end{aligned}$$

Then, the configuration of the M vortex dipoles (18) along the lines of latitudes Θ_1 and $2\pi - \Theta_1$ is a relative equilibrium moving in the longitudinal direction with speed $V_M^d(\Theta_1)$.

Proposition 3.4. *Let $r_e = \exp(r_c(\Theta_1) - r_c(2\pi - \Theta_1))$ and $V_M^s(\Theta_1)$ be defined by*

$$\begin{aligned} V_M^s(\Theta_1) &= -\frac{\Gamma}{(R - r\cos\Theta_1)^2}\sum_{j=1}^{M}\left[\frac{K(r_e\exp(i\frac{2\pi}{M}j + i\frac{\pi}{M})) + K(r_e\exp(-i\frac{2\pi}{M}j - i\frac{\pi}{M})) - 1}{4\pi}\right] \\ &\quad + \frac{M\Gamma(r_c(\Theta_1) - r_c(2\pi - \Theta_1))}{4\pi^2\mathcal{A}(R - r\cos\Theta_1)^2} + \frac{\Gamma\sin\Theta_1}{4\pi(R - r\cos\Theta_1)^2}. \end{aligned}$$

Then the configuration of the staggered M rings (19) along the lines of latitudes Θ_1 and $2\pi - \Theta_1$ is a relative equilibrium moving in the longitudinal direction with speed $V_M^s(\Theta_1)$.

In [56], more vortex crystals are provided with the linear algebraic formulation. With the third method, we obtain the following vortex equilibria.

- (Longitudinal vortex rings) Suppose that N point vortices are polygonally arranged along the line of longitude $\phi = 0$. Owing to the discrete longitudinal rotational symmetry by the angle $\gamma_0 = 2\pi/N$, their locations are specified by

$$\vartheta_m = \frac{2\pi}{N}(m-1) + \gamma, \qquad \varphi_m = 0, \qquad m = 1, \ldots, N, \qquad \gamma \in [0, \gamma_0). \tag{20}$$

  The configuration (20) is referred to as *a longitudinal N-ring*. As far as we have confirmed, longitudinal N-rings up to $N = 400$ are vortex crystals for any γ. See [56] for the strengths of the point vortices. Figure 1(a) is an illustration of a longitudinal 6-ring on the toroidal surface of $R = 3$ and $r = 1$ ($\alpha = 3.0$) embedded in 3D Euclidean space.

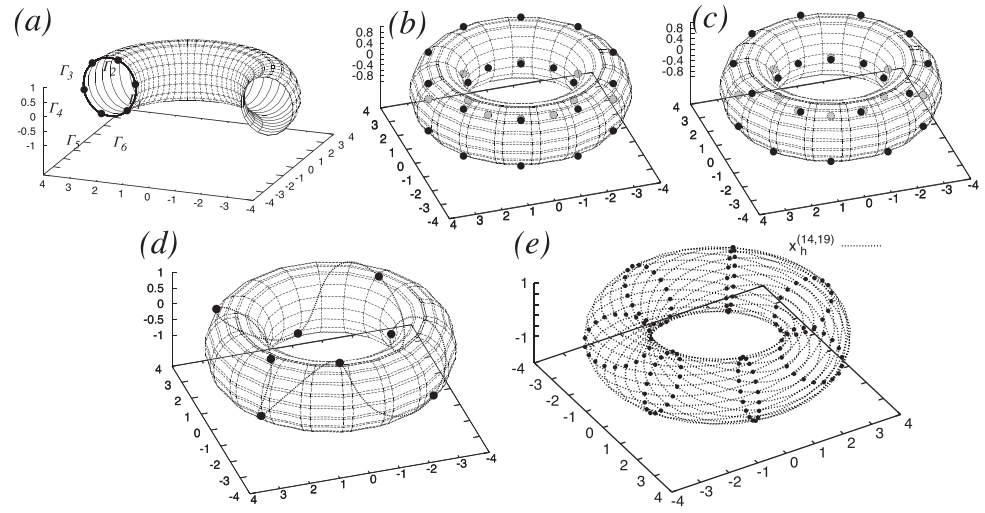

Figure 1: (a) A longitudinal 6-ring. (b) The 3-aligned 10-ring with $\gamma = 0$. (c) The 3-staggered 10-ring with $\gamma = 0$. (d) An asymmetric $N = 8$ point vortices on the helical line $\boldsymbol{x}_h^{(p,q)}$ with $p = 4$ and $q = 1$. (e) A point configuration of $L = 7$ helical longitudinal 19-rings aligned on the helical line $\boldsymbol{x}_h^{(p,q)}$ with $p = 14$ and $q = 19$.

- (K-aligned/staggered M-rings) For positive integers K and M, we consider the configuration where K latitudinal M-rings are arranged evenly in the latitudinal direction. Its configuration is specified by

$$\vartheta_{k,m} = \frac{2\pi}{K}(k-1) + \gamma, \quad \varphi_{k,m} = \frac{2\pi}{M}(m-1) + \Phi_k, \quad k = 1, \dots, K, \quad m = 1, \dots, M, \quad (21)$$

  in which $\gamma \in [0, \gamma_1)$, $\gamma_1 = 2\pi/K$ and $\Phi_k \in \mathbb{R}/2\pi\mathbb{Z}$ denote the longitudinal and latitudinal phase differences between M- rings respectively. For $\Phi_k = 0$, the configuration is called *a K-aligned M-ring*, while it is referred to as *a K-staggered M-ring* when $\Phi_k = \frac{2\pi}{M}(k \mod 2)$. We note that $N = KM$ is the total number of point vortices of this configuration. As examples, the 3-aligned 10-ring and the 3-staggered 10-ring for $\gamma = 0$ are shown in Figure 1(b) and (c) respectively. As far as we have examined, for any $\gamma \in [0, 2\pi/K)$ with $3 \leqq K \leqq 10$ and $3 \leqq M \leqq 10$, K-aligned/staggered M-rings are vortex crystals whose corresponding configuration matrices have a one-dimensional null-space. It is discussed that the limit of the configuration as $M \to 0$ for $K = 3$ becomes K (or $2K$) longitudinal "vortex sheets".

The Brownian ratchets scheme gives rise to asymmetric vortex crystals that are aligned along the helical curve $\boldsymbol{x}_h^{(p,q)}(s)$ for $p, q \in \mathbb{Z}$ on $\mathbb{T}_{R,r} \subset \mathbb{E}^3$,

$$\boldsymbol{x}_h^{(p,q)} : s \in \mathbb{R}/2\pi\mathbb{Z} \mapsto ((R - r\cos ps)\cos qs, (R - r\cos ps)\sin qs, r\sin ps) \in \mathbb{E}^3.$$

This curve is homotopic to a loop corresponding to the element of the fundamental group associated with the toroidal surface, which is denoted by $x^p y^q$ for the generators x and y. Letting N

point vortices move randomly along the curve, we find asymmetric vortex crystals. An example is shown in Figure 1(d). We can obtain more vortex crystals with a helical symmetry as follows. Let (p, q) be a given pair of coprime positive integers. We choose L lines of longitudes, say $\phi_\ell \in \mathbb{R}/2\pi\mathbb{Z}$ for $\ell = 1, \ldots, L$. Then, each line ϕ_ℓ intersects with the helical curve $\boldsymbol{x}_h^{(p,q)}$ at q points. We thus obtain $N = Lq$ point configurations aligned along the helical curve, which is referred to as longitudinal helical q-rings. By the Brownian ratchets for the lines of longitudes $\{\phi_\ell\}_{\ell=1}^N$, we observe numerically that, for a certain pair of (p, q), there exists a real $\gamma_L^{(p,q)}$ such that the longitudinal helical q-rings at $\phi_\ell = \frac{2\pi}{L}(\ell - 1) + \gamma_L^{(p,q)}$ for $\ell = 1, \ldots, L$ form a vortex crystal. One example is shown in Figure 1(e). See more longitudinal helical q-rings in [56] and its supplemental material. Moreover, a systematic numerical investigation yields the following conjecture.

Conjecture 3.1. *Let L and q be prime numbers, and $p < q$ be multiples of L given above. Then there exists a real $\gamma_L^{(p,q)} \in [0, 2\pi/L)$ such that L longitudinal q-rings consisting of the intersection points between the helical curve $\boldsymbol{x}_h^{(p,q)}$ and the lines of latitude $\phi_\ell = \frac{2\pi}{L}(\ell - 1) + \gamma_L^{(p,q)}$ form a vortex crystal.*

Let us briefly comment on the linear stability of the vortex crystals. We discuss in Section 3.4 the stability of the latitudinal N-ring configuration in detail. On the other hand, it is numerically confirmed that most of the vortex crystals obtained the third/fourth approaches are linearly unstable.

3.3 Interactions of two point vortices

We examine in [53] how two point vortices interact with each other. When the two point vortices are put in the unbounded plane and on the surface of a sphere without boundaries, the interactions between the two point vortices are well-understood. For instance, the identical vortex pair with $\Gamma_1 = \Gamma_2$ co-rotates around their centre point at a constant speed without changing the relative distance. On the other hand, the vortex dipole with $\Gamma_1 = -\Gamma_2$ on these surfaces propagates together along the geodesics at a constant speed without changing relative distance. We here observe the interaction of two point vortices on the surface of a torus with the vortex dynamics model.

Since the 2-vortex system is integrable, we reduce the original system into a one-degree-of-freedom Hamiltonian system with using the two invariants $\mathcal{H}$ and I_N. It is first shown that the evolution of the vortex dipole is defined globally in time.

Theorem 3.2. *The vortex dipole on the toroidal surface never collides.*

In addition, we obtain the following symmetry with respect to the evolution of the vortex dipole.

Lemma 3.1. *$\forall t \in \mathbb{R}$, $\theta_1(t) = \theta_2(t)$ and $\phi_1(t) + \phi_2(t) = 0$ holds if and only if $\exists t_0 \in \mathbb{R}$, $\theta_1(t_0) = \theta_2(t_0)$ and $\phi_1(t_0) + \phi_2(t_0) = 0$.*

This lemma indicates that when the vortex dipole is set on the same line of latitude at the initial moment, the latitudinal components of the two point vortices remain the same for all time. Substituting this relation into the Hamiltonian, we obtain a reduced Hamiltonian, which is a function of θ_1 and ϕ_1. Since every contour line of the reduced Hamiltonian corresponds to an orbit of the vortex dipole, we can classify the evolution of the vortex dipole by choosing appropriate values of the Hamiltonian as we see in Figure 2(a). We find that the distance between the two point vortices is not always constant. In addition, the topological structure of orbits changes as

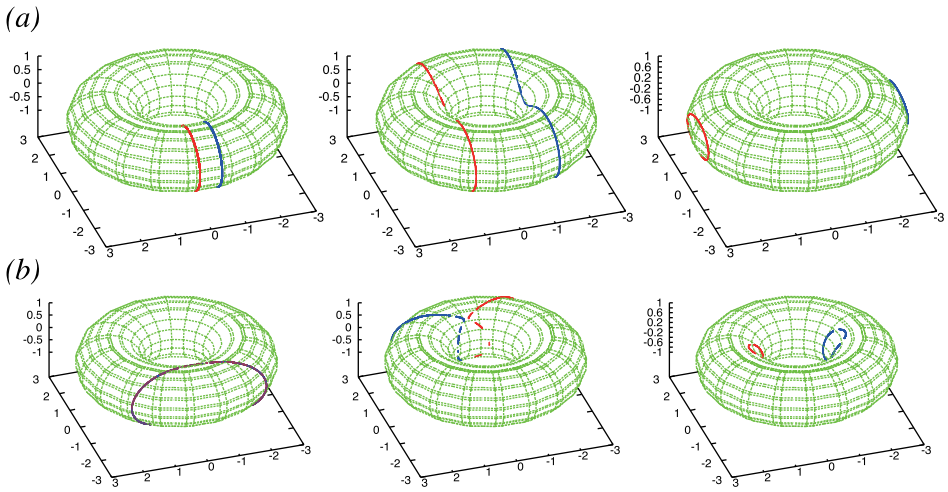

Figure 2: (a) Evolutions of the vortex dipole. (b) Evolutions of the identical vortex pair.

the initial distance between them increases. That is to say, when the two point vortices are close to each other, the vortex dipole moves around the handle, whose orbits are homotopic to irreducible curves. As the distance increases, the orbits of the vortex dipole become reducible. This change occurs as s a consequence of the existence of a handle structure.

For the identical point vortices, we have not yet proven the global existence of the solution, although the 2-vortex system is integrable. On the other hand, we can reduce the system into a one-degree-of-freedom Hamiltonian system by using the first integral I_N. By choosing several contour lines of the reduced Hamiltonian, we observe the orbits corresponding to these contours. Some examples are shown in Figure 2(b). The interaction of the identical point vortices is more complicated than the vortex dipole. We see a co-rotating orbit as shown in the left panel of the figure, which is similar to those of the identical vortex pair in unbounded plane and on the spherical surface. On the other hand, for some other values of the Hamiltonian, the two point vortices go along repulsive orbits around the handle (in the middle panel), or two independent rotating orbits around the antipodal locations (in the right panel).

3.4 Linear stability of a latitudinal N-ring point vortices

As we mentioned in Section 3.2, most of the vortex crystals obtained in Section 3.1 are linearly unstable. However, the stability of the N-ring on the line of latitude Θ_0 changes depending on the latitude Θ_0 and the modulus $\alpha = R/r$. We summarize the linear stability analysis of the N-ring carried out in [54]. Introducing small perturbations to the N-ring configuration,

$$\theta_m(t) = \Theta_0 + \varepsilon\vartheta_m(t), \qquad \phi_m(t) = \frac{2\pi m}{N} + tV_N(\Theta_0) + \varepsilon\varphi_m(t), \qquad \varepsilon \ll 1,$$

we derive the linearized equation for the perturbations $\vartheta_m(t)$ and $\varphi_m(t)$. We obtain all eigenvalues $\lambda_0^{\pm} = 0$, $\lambda_p^{\pm}$ for $p = 1, \ldots, N$ and their corresponding eigenvectors of the linearized matrix explicitly, from which we have the following stability criterion.

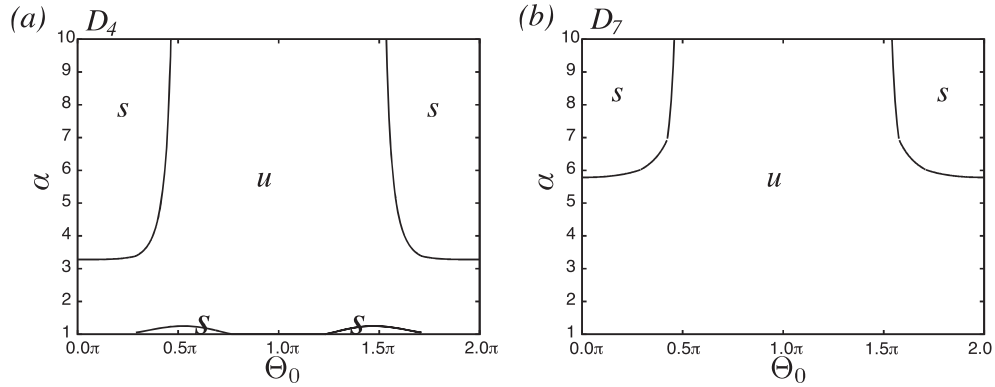

Figure 3: Stability region D_N for the N-ring. The components represented by "s" (resp. "u") is the parameter region where the N-ring becomes neutrally stable (resp. linearly unstable). (a) D_4. (b) D_7.

Proposition 3.5. *The N-ring is neutrally stable if and only if*

$$\Lambda_p^{(N)} \equiv p\left(1-\frac{p}{N}\right)+\frac{2p\rho^p}{1-\rho^p} \leqq (\alpha-\cos\Theta_0)\left(\frac{\alpha-\cos\Theta_0}{\pi\alpha}+\frac{\cos\Theta_0}{N}-\frac{8\pi r^2 V_N(\Theta_0)\sin\Theta_0(\alpha-\cos\Theta_0)}{N\Gamma}\right)$$

is satisfied for all $p=1,\dots,N-1$.

In other words, the condition is equivalent to say that if

$$\max_{p=1,\dots,N-1}\Lambda_p^{(N)} \leqq (\alpha-\cos\Theta_0)\left(\frac{\alpha-\cos\Theta_0}{\pi\alpha}+\frac{\cos\Theta_0}{N}-\frac{8\pi r^2 V_N(\Theta_0)\sin\Theta_0(\alpha-\cos\Theta_0)}{N\Gamma}\right) \quad (22)$$

holds, then the N-ring is neutrally stable. Note that the criterion depends on the two parameters (Θ_0,α) for given N. Hence, in order to discuss the linear stability of the N-ring, we show in Figure 3 the stability region, say $D_N(\Theta_0,\alpha)$, which is defined by

$$D_N = \{(\Theta_0,\alpha)\in\mathbb{R}/2\pi\mathbb{Z}\times(1,\infty)\,|\,\Theta_0 \text{ and } \alpha \text{ satisfy } (22)\}\,.$$

In this figure, the domains with the symbol "s" represent the domain of stability, while that with "u" is the parameter region where the N-ring becomes linearly unstable. The region is symmetric with respect to $\Theta_0=\pi$. First, we observe small connected components of D_4 in the neighborhood of $(\Theta_0,\alpha)=(\pi/2,1)$ and $(3\pi/2,1)$, while they no longer exist in D_7. Next, in both of D_4 and D_7, we find that there exists an aspect ratio, say $\alpha_0(N)$, such that a connected component of D_N exists inside the region $(\Theta_0,\alpha)\in[0,\pi/2)\times[\alpha_0(N),\infty)\cup(3\pi/2,2\pi]\times[\alpha_0(N),\infty)$. The boundaries of these components tend to the lines $\Theta_0=\pi/2$ and $\Theta_0=3\pi/2$ as $\alpha\to\infty$. This indicates that the N-rings located at the inner side of the toroidal surface is neutrally stable, while those on the outer side are linearly unstable. Also, we see $\alpha_0(4)<\alpha_0(7)$. As a matter of fact, we have observed numerically that $\alpha_0(N)$ is monotonically increasing as N gets larger. This indicates that, for every fixed α, the N-ring on the surface of a torus with the aspect ratio α becomes linearly unstable for sufficiently large N. The observations above are confirmed mathematically as follows.

For sufficiently small $\alpha>1$, we show the existence of the small connected components in the stability region for $2\leqq N\leqq 6$.

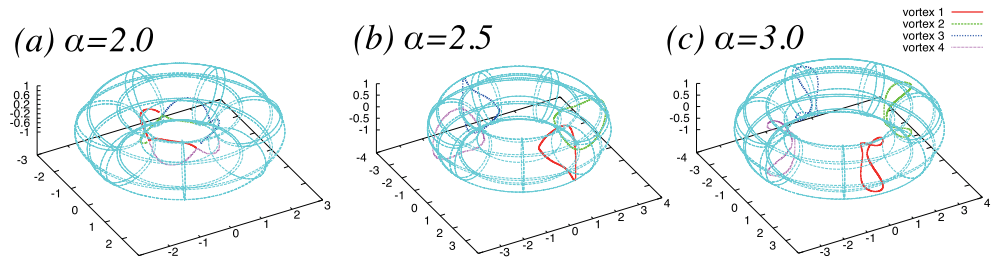

Figure 4: Examples of unstable periodic orbits of a perturbed 4-ring.

Theorem 3.3. *For sufficiently small $\varepsilon_0 > 0$ and for any α satisfying $1 + \varepsilon_0 > \alpha > 1$, there exists $\delta > 0$ such that for all $\Theta_0 \in (\pi/2 - \delta, \pi/2 + \delta) \cup (3\pi/2 - \delta, 3\pi/2 + \delta)$, the N-ring is neutrally stable if $2 \leqq N \leqq 6$, and unstable if $N \geqq 7$.*

This result is closely related to the classical results on the linear stability of the N-ring in the unbounded plane and on the spherical surface: It has been shown in [20, 62] that the N-ring in the plane is neutrally stable for $N \leqq 7$ and unstable for $N > 7$. A stability analysis of the N-ring on a line of latitude of the sphere reveals that the N-ring around the pole is nonlinearly stable for $N < 7$, neutrally stable for $N = 7$ and unstable for $N > 7$, although the stability depends largely on the line of latitude where they are placed [49]. For sufficiently small $\alpha \gtrapprox 1$, the stability of the N-ring around $\Theta_0 = \pi/2$ and $3\pi/2$, where Gauss curvature is zero, is similar to the planar and the spherical cases.

For fixed α and Θ_0, the following claims that the N-ring becomes linearly unstable for sufficiently large number of N.

Theorem 3.4. *For all $\alpha > 1$ and $\Theta_0 \in [0, 2\pi)$, there exists $N_0(\Theta_0, \alpha) \geqq 1$ such that the N-ring is unstable for all $N \geqq N_0$.*

The final result indicates that, for any N, there exists $\alpha_0(N) > 1$ such that the N-ring on the toroidal surface with the spect ratio $\alpha > \alpha_0(N)$ is linearly unstable.

Theorem 3.5. *For all $N \geqq 2$, $p = 1, \ldots, N-1$ and $\Theta_0 \in [0, 2\pi)$, there exists $\alpha_0 > 1$ such that for all $\alpha \geqq \alpha_0$ the following holds.*

1. $\Theta_0 \in [0, 2\pi) \setminus [\pi/2, 3\pi/2] \Longrightarrow \operatorname{Re} \lambda_p^{\pm} = 0$;
2. $\Theta_0 \in (\pi/2, 3\pi/2) \Longrightarrow \operatorname{Re} \lambda_p^{+} > 0 > \operatorname{Re} \lambda_p^{-}$;
3. $\Theta_0 = \pi/2, 3\pi/2$ *and* $p \geqq 2 \Longrightarrow \operatorname{Re} \lambda_p^{\pm} = 0$;
4. $\Theta_0 = \pi/2, 3\pi/2$ *and* $p = 1 \Longrightarrow \operatorname{Re} \lambda_p^{+} > 0 > \operatorname{Re} \lambda_p^{-}$.

In the same paper [53], the evolution of the linearly unstable N-ring under a small perturbation is also considered. Since the N point vortex system is not integrable for $N \geqq 3$, the evolution of the perturbed N-ring is chaotic in general. However, owing to a discrete symmetry of the N-ring, one can obtain some unstable periodic orbits by restricting the Hamiltonian system with N degrees of freedom into a reduced Hamiltonian system with one degree of freedom. Figure 4 shows some unstable periodic orbits when the 4-ring is perturbed in the reduced 2-dimensional phase space. When the aspect ratio changes, each orbit of the point vortex is homotopic to a longitudinal curve (Figure 4(a)), a latitudinal curve (Figure 4(b)) and a point (Figure 4(c)).

4 Steady solution of Stuart-type vortex distribution

We consider a continuous distribution of the Stuart-type vortex on the toroidal surface, satisfying the following modified Liouville equation [55].

$$\nabla^2_{\mathbb{T}_{R,r}}\psi = ce^{d\psi} + g(\zeta), \quad c, d \in \mathbb{R}, \quad cd < 0.$$

The functional form of $g(\zeta)$ is determined so that the solution of this equation is induced from that of the Liouville equation in the plane, $\nabla^2_{\mathbb{R}^2}\psi_p = ce^{d\psi_p}$, which is expressed as follows [15]:

$$\psi_p(\zeta, \overline{\zeta}) = \frac{1}{d}\log\left[\frac{2|f'(\zeta)|^2}{-cd(1+|f(\zeta)|^2)}\right],$$

where $f(\zeta)$ is a given analytic function on $\mathbb{C}$. After some calculations, we find that the function $g(\zeta)$ is equivalent to Gauss curvature of the toroidal surface,

$$g(\theta) = -\frac{2}{d}\frac{\cos\theta}{r(R-\cos\theta)} \equiv \frac{2}{d}\kappa(\mathbb{T}_{R,r}).$$

Let us remember that the functional form of $g(\zeta)$ for Stuart vortex on the surface of the unit sphere is given by $\frac{2}{d}$. This is consistent with the present result, since the curvature of the spherical surface is $\kappa(\mathbb{S}^2) = 1$. We thus obtain the analytic formula of the modified Liouville equation as follows.

$$\psi(\zeta, \overline{\zeta}) = \psi_p(\zeta, \overline{\zeta}) - \frac{2}{d}\log\left[\frac{R - r\cos\theta}{2|\zeta|}\right] = \psi_p(\zeta, \overline{\zeta}) - \frac{2}{d}\log\lambda(\zeta, \overline{\zeta}), \tag{23}$$

where $\lambda(\zeta, \overline{\zeta})$ is the conformal factor associated with the metric of the toroidal surface. We also note that the analytic solution for Stuart vortex on the surface of the unit sphere [16] is represented by the same formula with the conformal factor of the surface, i.e., $\lambda = (1+|\zeta|^2)^2$. Let us also remark that the existence of the modification function does not affect Gauss' constraint (2) in this case, since Gauss-Bonnet theorem assures the total curvature over the toroidal surface vanishes:

$$\iint_{\mathbb{T}_{R,r}} \kappa(\mathbb{T}_{R,r})d\sigma = 2\pi\chi(\mathbb{T}_{R,r}) = 0,$$

where $\chi(M)$ denotes the Euler characteristics of the manifold M. Hence, after the explicit solution (23) is obtained by specifying the analytic function $f(\zeta)$, we then confirm that the following Gauss' condition is satisfied.

$$\iint_{\mathbb{T}_{R,r}} e^{d\psi}d\sigma = 0.$$

The choice of the analytic function $f(\zeta)$ is not arbitrary when we consider the solution on the toroidal surface, since the function is not only analytic on the annular domain $\mathcal{D} = \{\zeta \in \mathbb{C} \,|\, \rho < |\zeta| < 1\}$, but it should also be doubly periodic with respect to $\theta \mapsto \theta \pm 2m\pi$ and $\phi \mapsto \phi \pm 2n\pi$ for any $n, m \in \mathbb{Z}$. Stuart [59] used $f(\zeta) = \tan(z) = \sin(z)/\cos(z)$ to construct a solution in the plane with the periodic boundary condition. We extend the choice of the function to the doubly periodic case. That is to say, introducing the conformal mapping $\zeta = e^z$ from $\mathcal{D}$ to $\mathcal{D}_z = \{z \in \mathbb{C} \,|\, -2\pi\mathcal{A} \leqq \mathrm{Re}z \leqq 0, 0 \leqq \mathrm{Im}z \leqq 2\pi\}$, which is a rectangular fundamental domain, we choose the analytic function as follows.

$$f(z) = \frac{\mathrm{sn}(z)}{\mathrm{cn}(z)} = \frac{\mathrm{sn}(\log\zeta)}{\mathrm{cn}(\log\zeta)},$$

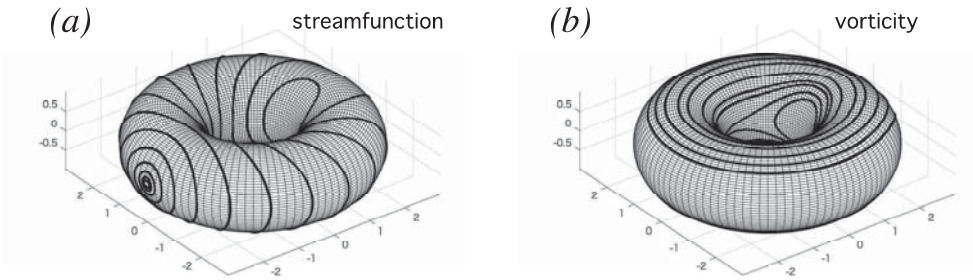

Figure 5: Solution of the Liouville equation with Stuart-type vorticity distribution on the surface of a torus with the aspect ratio $\alpha = 2.0$. (a) Stream-function and (b) vorticity.

in which $\mathrm{sn}(z)$ and $\mathrm{cn}(z)$ are the Jacobi elliptic functions with the quarter periods $K = \pi\mathcal{A}$ and $K' = \pi$. Plugging it into the formula (23), we obtain the solution

$$\psi(\zeta, \overline{\zeta}) = \frac{1}{d} \log \left[-\frac{2|\mathrm{dn}(\log \zeta)|^2}{cd(|\mathrm{sn}(\log \zeta)|^2 + |\mathrm{cn}(\log \zeta)|^2)^2 (R - r\cos\theta)^2} \right].$$

The function

$$w(z, \overline{z}) = \frac{|\mathrm{dn}(z)|^2}{(|\mathrm{sn}(z)|^2 + |\mathrm{cn}(z)|^2)^2}$$

in this formula is doubly periodic with respect to $z \mapsto z + 2K$ and $z \mapsto z + 2iK'$ with $K = \pi\mathcal{A}$ and $K' = \pi$. We also find that the function has two simple zeros at $\alpha_1 = iK' = \pi$ and $\alpha_2 = K + iK' = \pi\mathcal{A} + \pi i$ in the fundamental domain $\mathcal{D}_z$. Since the complex potential for a point vortex at $z = \alpha$ is locally represented by $\psi(z, \overline{z}) \sim -\frac{\Gamma}{2\pi} \log|z - \alpha|$, there exist two point vortices with the identical strength $-4\pi/d$ at $z = \alpha_1$ and α_2, which correspond to the antipodal locations on the toroidal surface. Since two point vortices located at the antipodal positions are always vortex crystal for arbitrary strengths as we see in Section 3.1, the formula yields the steady solution on the surface of a torus. It is also shown that the solution satisfies Gauss' constraint (2). Figure 5 shows the stream-function and the vorticity distribution of the solution on the toroidal surface with the aspect ratio $\alpha = 2.0$.

5 Summary and future direction

In this review article, we have introduced several recent results on vortex dynamics on the surface of a torus. The model equation is derived based on the mathematical formulation starting from Poisson's equation for the stream-function and the vorticity. For vorticity distributions such as point vortices and Stuart-type vorticity distribution, we have constructed the stream-function explicitly. With this model, we consider the problems finding vortex crystals, which is a critical point of the Hamiltonian containing a logarithmic particle-interaction energy. The linear stability of vortex crystals and the interactions between point vortices are also discussed. Moreover, we find

an analytic formula of a modified Liouville equation on the surface of a torus, which is the counterpart of Stuart vortex with a continuous vorticity distribution. One issue of this mathematical derivation is that we don't take the circulation theorem around the handle into considerations in this mathematical formulation when we allow point vortices to move. In order to make this model satisfy the circulation theorem, we may need to introduce a certain external flow, called "pore flow" as discussed in [14, 39]. In connection with the configurations of quantized vortices, as shown in [56], the strengths of the vortex crystals except the antipodal vortex crystals and the N-ring cannot be normalized as an integer generically. In this sense, vortex crystals fail to have quantized strengths. This may be remedied by combining point vortices with the Stuart-type vortex distributions as considered in [35]. It will be a future direction of the present study.

Let us finally comment on the relation between the minimizing point configurations and vortex crystals on compact surfaces. The point configurations of the vortex crystals are spreading in the longitudinal as well as latitudinal directions evenly, which are different from the point configurations minimizing the Riesz energy, although the Hamiltonian (9) has a logarithmic singularity as $\mathcal{E}_0(A, N)$. Investigating the relation between the enery-minimizing point configurations and vortex crystals will also be another interesting future topic.

Acknowledgements

The author is partially supported by JSPS Kakenhi(B) no. 18H01136. This work was also partially supported by a grant from the Simons Foundation. The author would like to thank the Isaac Newton Institute for Mathematical Sciences for support and hospitality during the programme [CAT] when work on this paper was undertaken, which was supported by: EPSRC grant number EP/R014604/1.

References

[1] Abo-Shaeer, J. R., Raman, C., Vogels, J. M. and Ketterle, W. 2001 *Observation of vortex lattices in Bose-Einstein Condensates.* Science **292** pp. 476–479.

[2] Abrikosov, A. A. 1955 *On the magnetic properties os superconductors of the second group.* Soviet. Phys. J. Exp. Theor. Phys. **32** pp. 1442–1452.

[3] Abrikosov, A. A. 2003 *Nobel lecture: Type-II superconductors and the vortex lattice.* Rev. Mod. Phys. **76** pp. 975–979.

[4] Aref, H. and Vainchtein, D. L. 1998 *Point vortices exhibit asymmetric equilibria.* Nature **392** pp. 769–770. (doi:10.1038/33827)

[5] Aref, H., Newton, P. K., Stremler, M. A., Tokieda, T. and Vainchtein, D. L. 2003 *Vortex crystals.* Adv. Appl. Mech. **39** pp. 1–79.

[6] Bhutani, O. P., Moussa, M. H. M. and Vijayakumar, K. 1994 *On the generalized forms of exact solutions to the Liouville equation via direct approach.* Int. J. Eng. Sci. **32** pp. 1965–1969. (doi:10.1016/0020-7225(94)90092-2)

[7] Boatto, S. and Koiller, J. 2015 *Vortex on closed surfaces.* Fields Inst. Commun. **73** pp. 185–237. (doi:10.1007/978-1-4939-2441-7)

[8] Bogomolov, A. 1977 *Dynamics of vorticity at a sphere.* Izv. Acad. Sci. USSR Atmos. Oceanic Phys. **15** pp. 863–870. (doi:10.1007/BF01090320)

[9] Borodachov, S. V., Hardin, D. P. and Saff, E. B. 2007 *Asymptotics for discrete weighed minimal Riesz energy problems on rectifiable sets*. Trans. Amer. Math. Soc. **360** No. 3 pp. 1559–1580.

[10] Borodachov, S. V., Hardin, D. P. and Saff, E. B. 2007 *Asymptotics of best-packing on rectifiable sets*. Proc. Amer. Math. Soc. **135** No. 8 pp. 2369–238.

[11] Calogero, F. and Degasperis, A. 1982 *Spectral transform and solitons*. Amsterdam, Netherlands: North Holland.

[12] Campbell, L. J. and Ziff, R. 1978 *A Catalog of Two-Dimensional Vortex Patterns*. LA-7384-MS, Rev., Informal report, Los Alamos Scientific Laboratory.

[13] Campbell, L. J. and Kadtke, J. B. 1987 *Stationary Configurations of Point Vortices and Other Logarithmic Objects in Two dimensions*. Phys. Rev. Lett. **58** No.7 pp. 671–673.

[14] Corrada-Emmanuel, A. 1994 *Exact solution for superfluid film vortices on a torus*. Phys. Rev. Lett. **72** pp. 681–684. (doi:10.1103/PhysRevLett.72.681)

[15] Crowdy, D. G. 1997 *General solutions to the 2D Liouville equation*. Int. J. Eng. Sci. **35** pp. 141–149. (doi:10.1016/S0020-7225(96)00080-8)

[16] Crowdy, D. G. 2004 *Stuart vortices on a sphere*. J. Fluid Mech. **498** pp. 381–402. (doi:10.1017/ S0022112003007043)

[17] Damelin, S. B., Levesley, J., Ragozin, D. L. and Sun, X. 2009 *Energies, group-invariant kernels and numerical integration on compact manifolds*. J. Complexity **25** pp. 152–162.

[18] Damelin, S. B., Hickernell, F. J., Ragozin, D. L. and Zeng, X. 2010 *On energy, discrepancy and group invariant measures on measurable subsets of Euclidean space*. J. Fourier Anal. Appl. **16** pp. 813–839. (doi: 10.1007/s00041-010-9153-2)

[19] DiBattista, M. T. and Polvani, L. M. 1998 *Barotropic vortex pairs on a rotating sphere*. J. Fluid Mech. **358** pp. 107–133. (doi:10.1017/S0022112097008100)

[20] Dritschel, D. G. 1985 *The stability and energetics of co-rotating uniform vortices*. J. Fluid Mech. **157** pp. 95–134.

[21] Dritschel, D. G. and Boatto, S. 2015 *The motion of point vortices on closed surfaces*. Proc. R. Soc. A **471** 20140890. (doi:10.1098/rspa.2014.0890)

[22] Engels, P., Coddington, I., Haljan, P. C. and Cornell, E. A. 2002 *Nonequilibrium effects of anisotropic compression applied to vortex lattices in Bose-Einstein Condensates*. Phys. Rev. Lett. **89** No.10 100403 (doi:10.1103/PhysRevLett.89.100403)

[23] Engels, P., Coddington, I., Haljan, P. C., Schweikhard, V. and Cornell, E. A. 2003 *Observation of long- lived vortex aggregates in rapidly rotating Bose-Einstein condensates*. Phys. Rev. Lett. **90** No. 17 170405. (doi: 10.1103/PhysRevLett.90.170405)

[24] Essmann, U. and Träuble, H. 1967 *The direct observation of individual flux lines in type II superconductors*. Phys. Rev. Lett. **24**A No.10 pp. 526–527.

[25] Feynmann, R. P. 1955 *Application of Quantum Mechanics to Liquid Helium*. Prog. Low Temp. Phys., edited by D. F. Brewer (North-Holland, Amsterdam) **1** Chap. II. pp. 17–53.

[26] Fine, K. S., Cass, A. C., Flynn, W. G. and Driscoll, C. F. 1995 *Relaxation of 2D turbulence and vortex crystal*. Phys. Rev. Lett. **75** No. 18 pp. 3277–3282.

[27] Green, C .C. and Marshall, J. S. 2012 *Green's function for the Laplace-Beltrami operator on a toroidal surface*. Proc. R. Soc. A **469** 20120479. (doi:10.1098/rspa.2012.0479)

[28] Grzybowski B. A., Stone, H. A. and Whitesides, G. M. 2000 *Dynamic self-assembly of magnetized, millimetre-sized objects rotating at a liquid-air interface*. Nature **405** pp. 1033–1036.

[29] Hally, D. 1980 *Stability of streets of vortices on surfaces of revolution with a reflection symmetry*. J. Math. Phys. **21** pp. 211–217. (doi:10.1063/1.524322)

[30] Jin, D. Z. and Dubin, D. H. E. 2000 *Characteristics of two-dimensional turbulence that self-organizes into vortex crystals*. Phys. Rev. Lett. **84** No. 7 pp. 1443–1446.

[31] Hardin, D. P. and Saff, E. B. 2004 *Discretizing manifolds via minimum energy points*. Notices Amer. Math. Soc. **51** pp. 1186–1194.

[32] Hardin, D. P. and Saff, E. B. 2005 *Minimal Riesz energy point configurations for rectifiable d-dimensional manifolds*. Adv. Math. **193** pp. 174–204.

[33] Kimura, Y. and Okamoto, H. 1987 *Vortex motion of a sphere*. J. Phys. Soc. Japan **56** pp. 4203–4206. (doi:10:1143/JPSJ.56.4203)

[34] Kimura, Y. 1999 *Vortex motion on surfaces with constant curvature*. Proc. Roy. Soc. Lond. A **455** pp. 245–259. (doi:10.1098/rspa.1999.0311)

[35] Krishnamurthy, V. S., Wheeler, M. H., Crowdy, D. G. and Constantin, A. 2019 *Steady point vortex pair in a field of Stuart-type vorticity*. J. Fluid. Mech. **874** R1. (doi:10.1017/jfm.2019.502)

[36] Lin, C. C. 1941 *On the motion of vortices in two-dimensions. I. Existence of the Kirchhoff-Routh function*. Proc. Natl Acad. Sci. USA **27** pp. 570–575. (doi:10.1073/pnas.27.12.570)

[37] Lin, C. C. 1941 *On the motion of vortices in two-dimensions. II. Some further investigations on the Kirchhoff-Routh function*. Proc. Natl Acad. Sci. USA **27** pp. 575–577. (doi:10.1073/pnas. 27.12.575)

[38] Liouville, J. 1853 *Sur léquation aux différenes partielles* $d^2 \log \lambda / dudv \pm \lambda / 2a^2 = 0$. J. Math. Pures et Appl. **18** pp. 71–72.

[39] Machta, J. and Guyer, R. A. 1988 *Superfluid films in porous media*. Phys. Rev. Lett. **60** No. 20 pp. 2054–2057.

[40] Nasser, M. S., Sakajo, T., Murid A. H. and Wei, L. K. 2015 *A fast computational method for potential flows in multiply connected coastal domains*. Japan J. Indust. Appl. Math. **32** pp. 205–236. (doi:10.1007/s13160-015-0168-6)

[41] Nelson, R., Protas, B. and Sakajo, T. 2017 *Linear feedback stabilization of point vortex equilibria near a Kasper Wing.* J. Fluid Mech. **827** pp. 21–154 (2017) (doi:10.1017/jfm2017.484)

[42] Newton, P. K. 2001 *The N-vortex problem, analytic techniques.* Applied Mathematical Science **145**. New York, New York: Springer.

[43] Newton, P. K. and Sakajo, T. 2007 *The N-vortex problem on a rotating sphere. III. Ring configurations coupled with a background field.* Proc. Roy. Soc. A **463** pp. 961–977. (doi:10.1098/rspa.2006.1802)

[44] Newton, P. K. and Chamoun, G. 2007 *Construction of point vortex equilibria via Brownian ratchets*, Proc. Roy. Soc. A **463** pp. 1525–1540. (doi:10.1098/rspa.2007.1832)

[45] Newton, P. K. and Sakajo, T. 2009 *Point vortex equilibria on the sphere via Brownian ratchets.* Proc. Roy. Soc. A **465** pp. 437–455. (doi:10.1098/rspa.2008.0203)

[46] Newton, P. K. and Chamoun, G. 2009 *Vortex lattice theory: a particle interaction perspective.* SIAM Review **51** No. 3 pp. 501–542.

[47] Newton, P. K. and Sakajo, T. 2010 *Point vortex equilibria and optimal packings of circles on sphere.* Proc. Roy. Soc. A **467** pp. 1468–1490. (doi:10.1098/rspa.2010.0368)

[48] Nitsche, I., Voigt, A. and Wensch, J. 2012 *A finite element approach to incompressible two-phase flow on manifolds.* J. Fluid Mech. **708** pp. 418–438. (doi:10.1017/jfm.2012.317)

[49] Polvani, P. M. and Dritschel, D. G. 1993 *Wave and vortex dynamics on the surface of a sphere.* J. Fluid Mech. **255** pp. 35–64.

[50] Saffman, P. G. 1993 *Vortex dynamics.* Cambridge, United Kingdom: Cambridge University Press.

[51] Sakajo T. 2009 *Equation of motion for point vortices in multiply connected circular domains.* Proc. Roy. Soc. A **465** pp. 2589–2611. (doi:10.1098/rspa.2009.0070)

[52] Sakajo, T. 2012 *Fixed equilibria of point vortices in symmetric multiply connected domains.* Phys. D **241** pp. 583–599. (doi:doi:10.1016/j.physd.2011.11.021)

[53] Sakajo, T. and Shimizu, Y. 2016 *Point vortex interactions on a toroidal surface.* Proc. Roy. Soc. A **472** 20160271. (doi:10.1098/rspa.2016.0271)

[54] Sakajo, T. and Shimizu, Y. 2018 *Toroidal geometry stabilizing a latitudinal ring of N point vortices on a torus.* J. Nonlinear Sci. **28** pp. 1043–1077. (doi:10.1007/s00332-017-9440-z)

[55] Sakajo, T. 2019 *Exact solution to a modified Liouville equation with Stuart vortex distribution on the surface of a torus.* Proc. Roy. Soc. A **475** 20180666. (doi: 10.1098/rspa.2018.0666)

[56] Sakajo, T. 2019 *Vortex crystals on the surface of a torus.* Phil. Trans. Roy. Soc. A **377** 20180344. (doi:10.1098/rsta.2018.0344)

[57] Smale, S. 2000 *Mathematical problems for the next century.* Mathematics: Frontiers and Perspectives, (V. Arnold, M. Aliyah, P. Lax, and B. Mazur, eds.) pp. 271–294. Providence, RI: AMS

[58] Sohn, S. I., Sakajo, T. and Kim, S. C. 2018 *Stability of barotropic vortex strip on a rotating sphere*. Proc. Roy. Soc. A **474** 2017883. (doi:10:1098.rspa.2017.0883)

[59] Stuart, J. T. 1967 *On finite amplitude oscillations in laminar mixing layers*. J. Fluid Mech. **29** No. 15 pp. 417–440. (doi:10.1017/S0022112067000941)

[60] Tammes, P. M. L. 1930 *On the origin of number and arrangements of the places of exit on the surface of pollen-grains*. Recl. Trav. Bot. Neerl. **27** pp. 1–84.

[61] Thomson, W. 1867 *On vortex atoms*. Phil. Mag. **34** pp. 15–24.

[62] Thomson, J. J. 1983 *A Treatise on the Motion of Vortex Rings*. New York: Macmillan.

[63] Turner, A. M., Vitelli, V. and Nelson, D. R. 2010 *Vortices on curved surfaces*. Rev. Mod. Phys. **82** pp. 1301–1348. (doi:10.1103/RevModPhys.82.1301)

[64] Yarmchuk, E. J. and Gordon, M. J. V. 1979 *Observation of stationary vortex arrays in rotating super-fluid helium*. Phys. Rev. Lett. **43** No. 4 pp. 214–217.